'Photogrammetric Week '95', D. Fritsch & D. Hobbie, Eds., Wichmann Verlag, Heidelberg, 1995

Earth Observation by means of SAR
Present State and Future Possibilities

PH. HARTL, K-H. THIEL, X. WU, Y. XIA, Stuttgart

ABSTRACT

Satellite SAR systems have shown up as excellent all weather remote sensing tool. The extension to interferometric and differential interferometric applications demonstrates complete new possibilities for Earth observation. A short introduction to the techniques is given and some typical applications are shown.

1. INTRODUCTION

Past

SAR - System	SEASAT	SIR-A	SIR-B	COSMOS
Country	USA	USA	USA	Russia
Freq. band / wavelength [cm]	L/23.5	L/23.5	L/23.5	S/10
Frequency [GHz]	1.275	1.275	1.275	3.0

Present

Locrosse	Almaz1-A	ERS-1	J-ERS-1	SIR-C/X-SAR	ERS-2
USA	Russia	ESA	Japan	USA/BRD	ESA
X/3.0	S/10	C/5.7	L/23.5	L,C,X	C/5.7
9.5	3.0	5.25	1.275	1.25; 5.3;9.6	5.25

Future

RADARSAT	ENVISAT-1	ALMAZ1-B	TRAVERS	EOS-SAR
Canada	ESA	Russia	Russia	USA
C/5,7	C/5.7	P,S,X/70,10,3.6	L,S/23,9.6	L,C,X
5.3	5.3	0.43; 3.1; 8.54	1.3; 3.1	1.25; 5.3; 9.6

Table 1: Satellite SAR systems.

The past, present and future SAR- systems for earth observation are listed in table 1. The SEASAT-mission demonstrated for the first time the extremely interesting features of a high resolution space-based imaging radar, which is able to map surface characteristics independent of clouds and daytime. The Shuttle missions SIR-A, -B applied the same type of L-band instrument in a lower orbit and demonstrated that the field of remote sensing and its application can be widely extended with SAR. The SIR-C/X-SAR Shuttle mission with the most powerful SAR-payload (multi-frequency, multi-polarisation and variable geometric illumination capabilities) was flown twice in 1995 and will most probably be flown again in 1997. The ERS-1 and ERS-2 satellites are presently both operating in the sun-synchronous orbit and deliver data sets in C-band. In the near future the Canadian RADARSAT will be launched, further extending the performance characteristics of the satellite SAR by introduction of additional operation modes (wide swath..). As can be seen from table 1, various other systems have been or will be flown. But in the following only results of the ERS-1/-2 mission and of the SIR-C/X-SAR mission will be presented, as they can well demonstrate the present state.

'Photogrammetric Week '95', D. Fritsch & D. Hobbie, Eds., Wichmann Verlag, Heidelberg, 1995

2. SAR- IMAGES

2.1 Intensity images

Normally SAR- images are "intensity-images". Each pixel represents in its brightness the power of the corresponding radar echo signal pixel by pixel. It depends on the backscatter feature of the surface element, which is a function of many frequency dependent parameters, such as surface roughness, electromagnetic characteristics of the material, wetness, polarization, incidence angle, geometric resolution, etc. A single "black and white" SAR-image of land surface is very often difficult to interpret. In most application areas one makes use, therefore, of combinations of either multi-temporal, or multi-frequency, or multi-polarisation images, or combinations hereof. Also integration with optical images and with GIS- related information is applied. Figure 1 shows examples of:

- seasonal/single frequency (L-Band),
- seasonal/single frequency (C-Band) and
- multi-frequency (L-, C- and X-Band)

image classification. Practical applications are possible in areas of vegetation mapping, crop monitoring, biomass estimation, monitoring of flooded areas, of soil moisture estimation, oil spill etc.

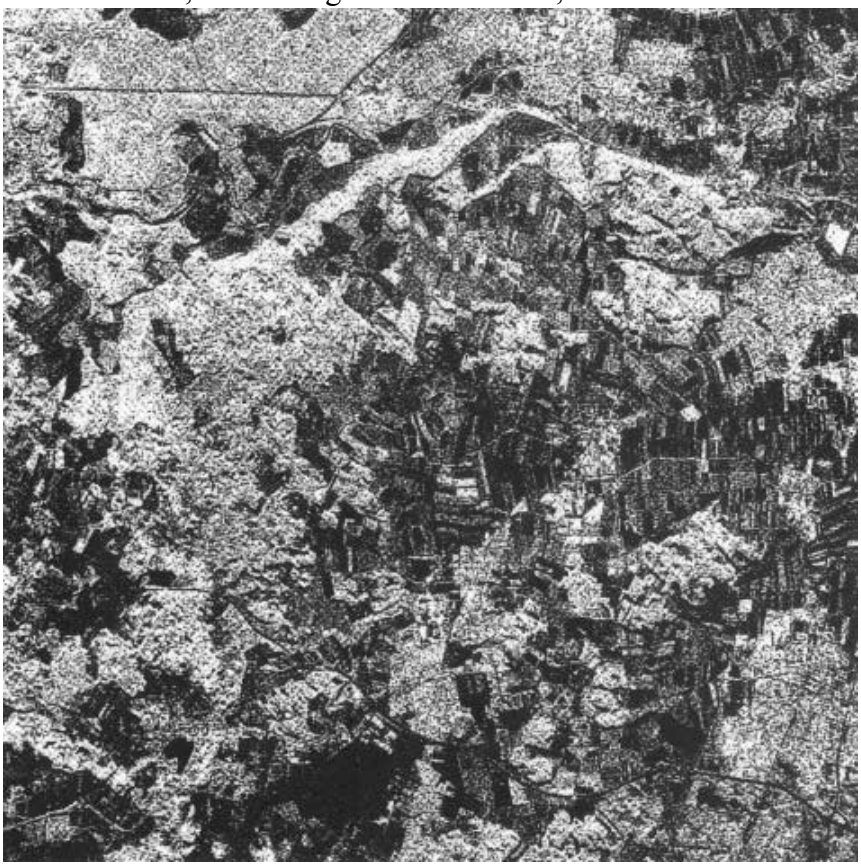

Figure 1a: Example of a L-Band SAR intensity image (Oberpfaffenhofen).

'Photogrammetric Week '95', D. Fritsch & D. Hobbie, Eds., Wichmann Verlag, Heidelberg, 1995

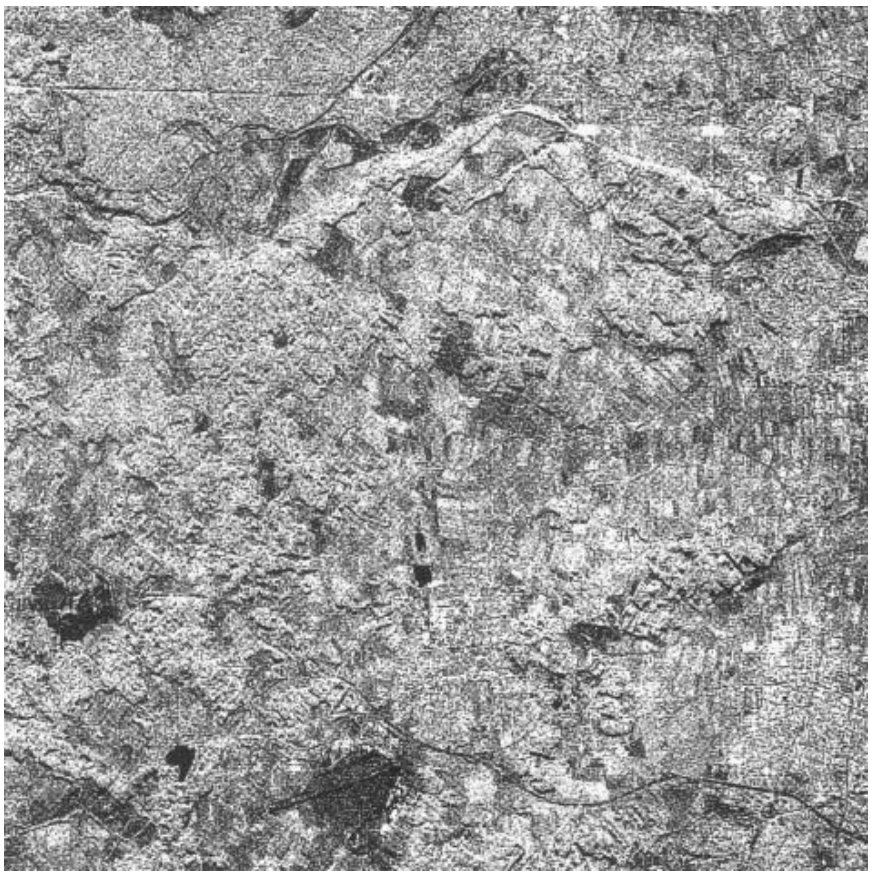

Figure 1b: Example of a C-Band SAR intensity image (Oberpfaffenhofen).

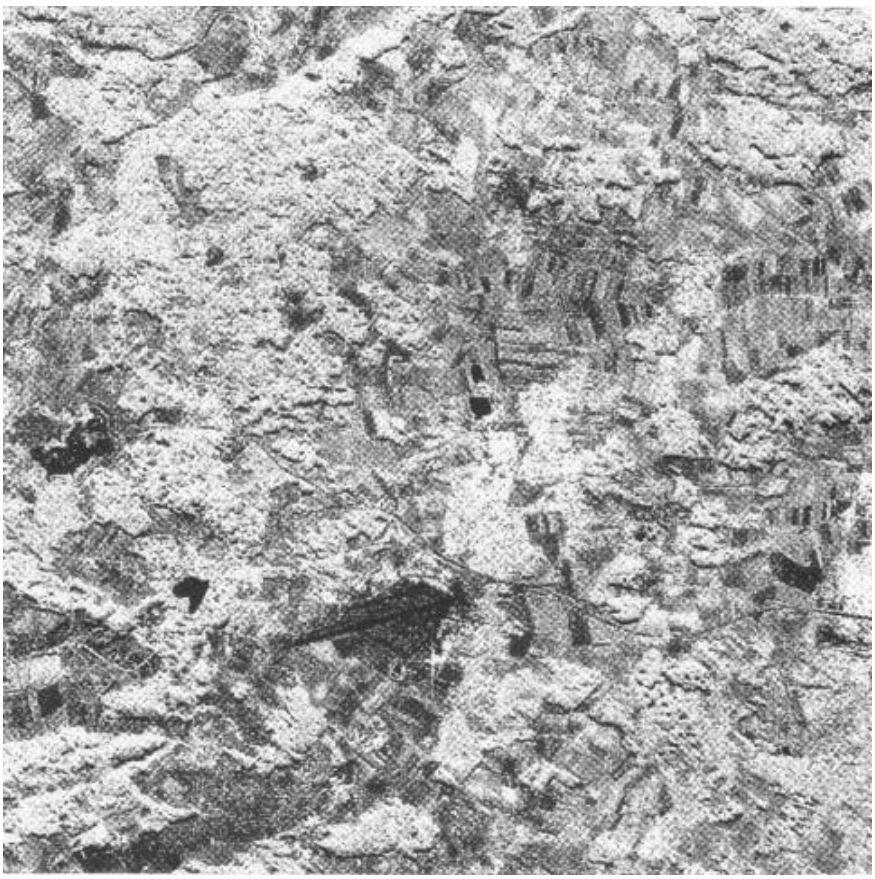

Figure 1c: Example of a multi-frequency SAR image (X-, C- and L-Band).

'Photogrammetric Week '95', D. Fritsch & D. Hobbie, Eds., Wichmann Verlag, Heidelberg, 1995

2.2 Interferometric images

If the same scene is imaged twice from the same satellite position, then one will receive identical intensity images, provided that nothing has changed in between the two instants of image acquisition. For scenes of a desert one can expect that such a situation will last for years, provided the corresponding meteorological conditions (no rain, no storm) exist and the surface would not change. In areas like Baden-Württemberg one could expect in a summer like 1995 that even within hours the backscatter characteristics will locally vary strongly. But let´s first assume that the variations are small enough. Then the difference of intensity on a pixel by pixel basis would be zero, if noise is neglected. If, however, the satellite positions concerning the first image and the second one differ, then the two images would become different in the brightness characteristics, because the backscatter characteristic of each pixel depends strongly on the incidence angle i of the SAR-signal. The sensitivity to the i-value is very strong and if the two SAR-imaging positions would differ by, say, $\Delta i = 30$ degrees, then it is very difficult, even for skilled people, to correlate the images precisely, because a bright spot can then change to become very dark and vice versa (speckle effect).
In the following, we assume, therefore to have a maximum distance of a few hundred meters between the two image acquisition positions ("baseline") compared to 875 km slant range distance. We can thus ignore the inclination influence.

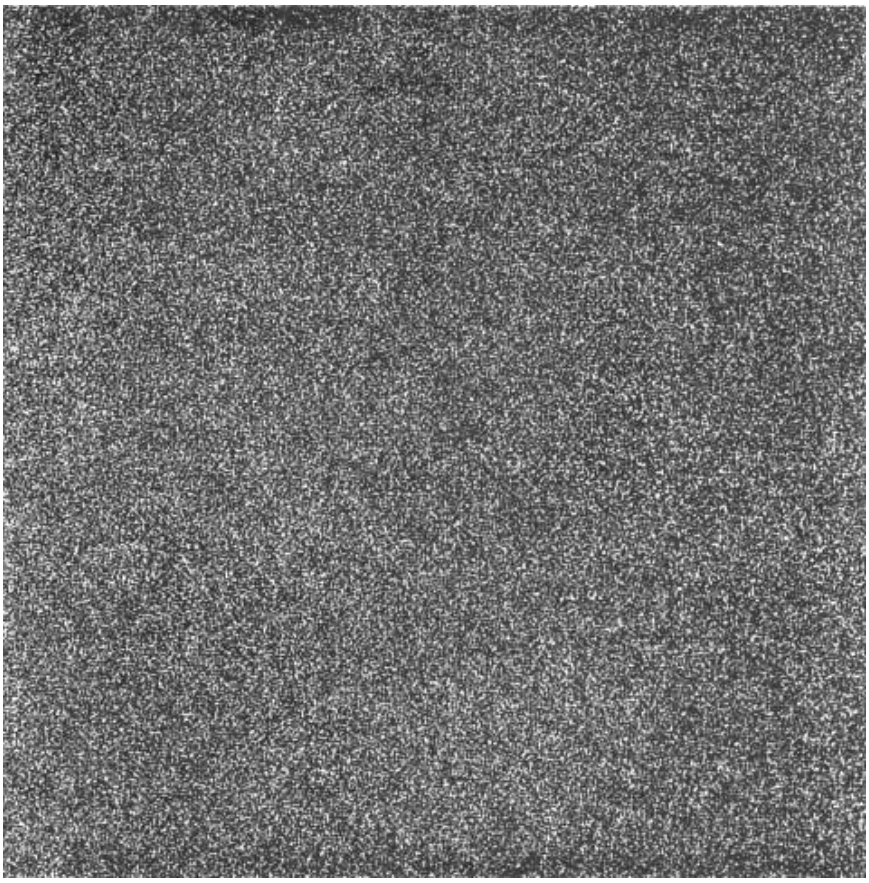

Figure 2: Phase image of a SAR-SLC scene.

Besides the intensity image we consider now the "phase-image". In the same manner as the intensity we can also map the "phase characteristic" of a single SAR- image as a brightness image (figure 2), with a grey-scale: very bright for phase-values of 2π and black for 0. The phase is the difference Φ between the microwave signal transmitted from the SAR and the received echo. This difference depends for each pixel from two factors: From the two-way range 2R between the satellite and backscattering element, and from the characteristically phase shift η of the surface of that element:

$\Phi = 2\pi \bullet 2R / \lambda + \eta$

η = phase shift value of backscattering element

The size of the backscattering ground element (pixel) with about 4 m by 20 m is very large compared to the wavelength of the SAR signal. This produces an almost random character of the "phase image". But taking a second image from the same position will produce an identical "phase image". As we assume that Δi is small enough not to vary the phase characteristics of the surface (η being identical in both images), it is obvious that the corresponding phase differences Φ_2, Φ_1 will only correspond to the range difference.

$$\Phi_2 - \Phi_1 = (2\pi X2R_2 / \lambda + \eta) - (2\pi X2R_1 / \lambda + \eta) = 4\pi X(R_2 - R_1) / \lambda .$$

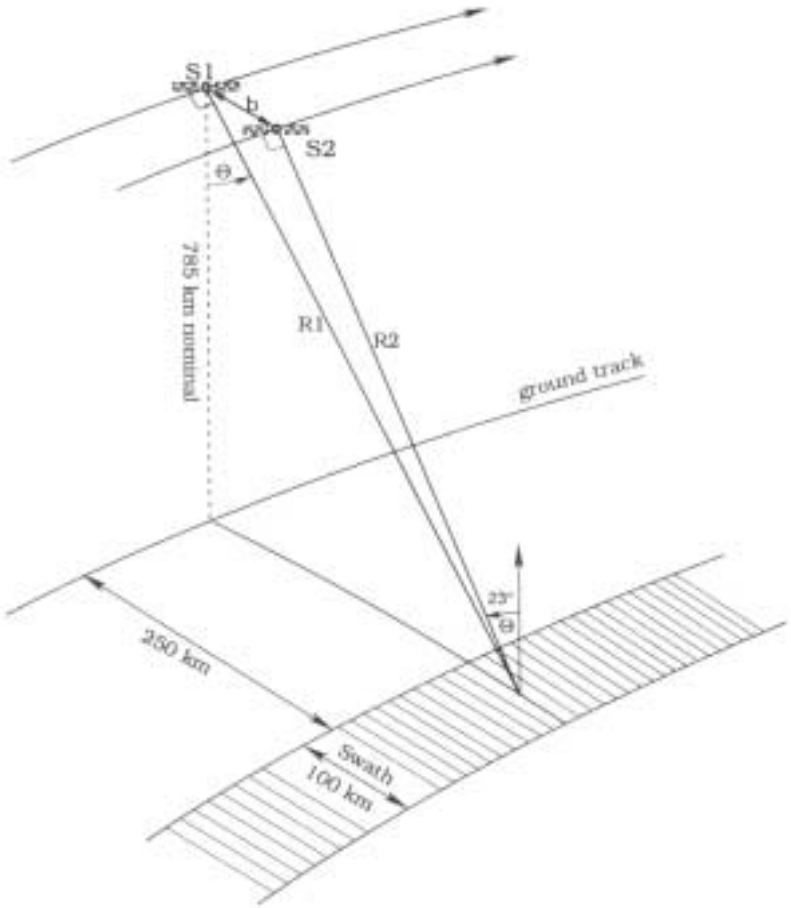

Figure 3: Satellite geometry with SAR interferometry.

2.3 Digital Elevation Model

Thus with respect to the satellite geometry (Figure 3) the phase difference from pixel to pixel in slant range direction is only changing slowly its value, generating "fringes" (Figure 4). The range difference also depends on the surface shape. If we want to determine the digital elevation model, then we can relate the whole geometry in various ways to the Geoid and deduct the corresponding value from the measured range difference ($R_2 - R_1$). In other words, we calculate theoretically the phase image with respect to the Geoid and deduct it from the measured one. The fringes of the Geoid will be deducted from the originally one measured and we will get the "relative phase" image, which will represent the relative height. Each of the "residue fringe" is a contour line of equal range difference. If we know from one of the points of the image the correct height, then we can calculate for the correct value for

'Photogrammetric Week '95', D. Fritsch & D. Hobbie, Eds., Wichmann Verlag, Heidelberg, 1995

all others, because one can show that the two neighbouring fringes differ in height e according to the equation

$$e = \frac{\Delta \Phi \cong \lambda}{4 \pi \left(\frac{B \cong H}{R \sqrt{R^2 \& H^2}} \right)} \qquad (1)$$

It is a function of the baseline and the wavelength (R and H are almost constant). For different frequencies we get for the same baseline different resolutions (Figure 5). A combination of images from different baselines or different frequencies can help to solve "phase ambiguity problems" when estimating the terrain height from the relative phase image. A correct integration of the "fringes" has to be performed.

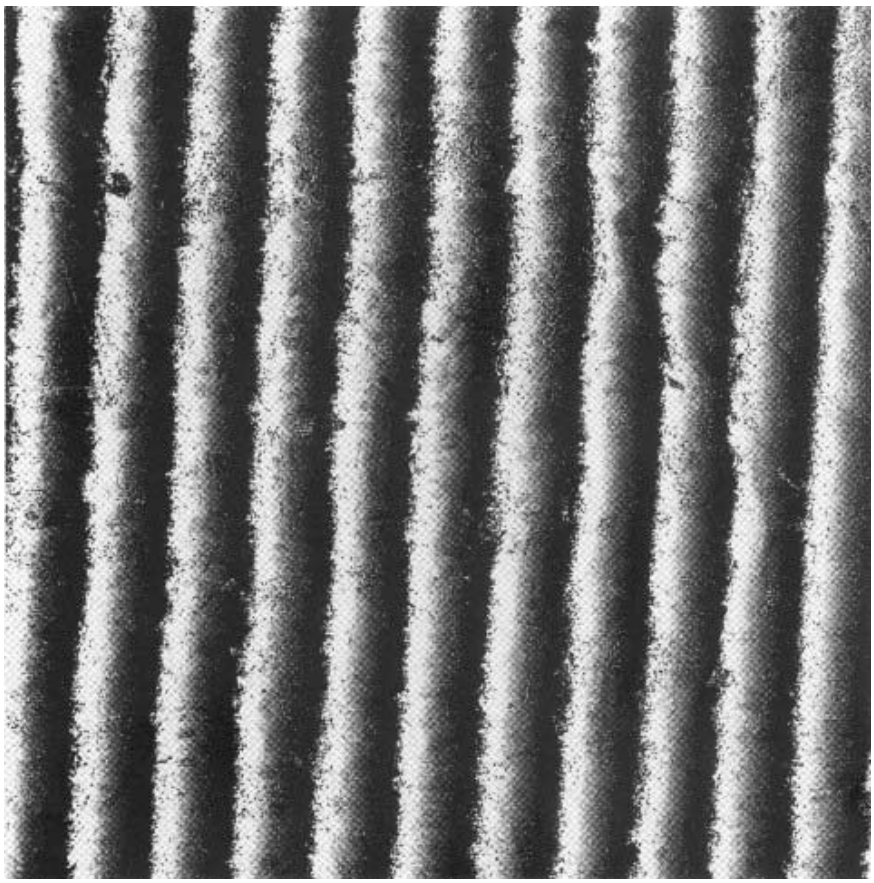

Figure 4: Fringe image of L-band SAR system of the area at Oberpfaffenhofen.

Different frequencies have also different penetrations into the surface: The C-band SAR, and the L-band SAR will, therefore have also different reference heights in forest, for example, the C-band height referring almost to the canopy, the L-band close to ground.

'Photogrammetric Week '95', D. Fritsch & D. Hobbie, Eds., Wichmann Verlag, Heidelberg, 1995

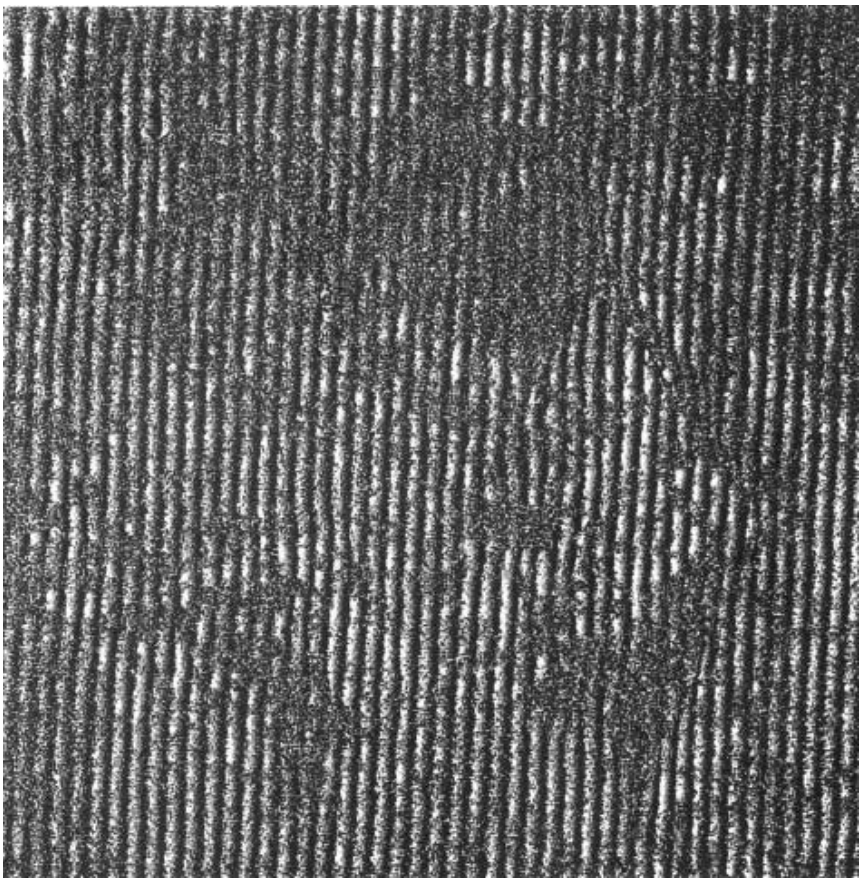

Figure 5: Fringe image of C-band SAR system of the area at Oberpfaffenhofen.

2.4 Differential SAR-Interferometry

The repeat orbit interferometry has the problem that a correct elevation model can only be expected, if nothing has changed between the first and the second image take. If a local change occurred, then this might be caused by either a geometric or a backscatter effect. The geometric effect can be locally, or regionally and the movement can be vertically, horizontally, or both ways. The local phase change might result from a change in material, or due to change in roughness etc. It could also be a time continuous motion or a sudden shift. The effect can be demonstrated simply by figure 6. Here the field work of farmers have changed the surface, producing clearly visible areas in the phase image.
Now we have many uncertainties. If we don´t recognise the changes then we interpret the phase difference as a DEM-feature and we get completely wrong height-values (e-values). If we identify it as a phase change, then we have still to solve, if it is a vertical or a horizontal effect, a continuous motion, or a sudden event etc. Misinterpretation concerning DEM errors can be excluded by using a third SAR-image with different baseline, or by another interferogramme for a different frequency. If a large elevation can be excluded, then we measure a dynamic effect with a sensitivity, which is equivalent to small fractions of half a wavelengths.

'Photogrammetric Week '95', D. Fritsch & D. Hobbie, Eds., Wichmann Verlag, Heidelberg, 1995

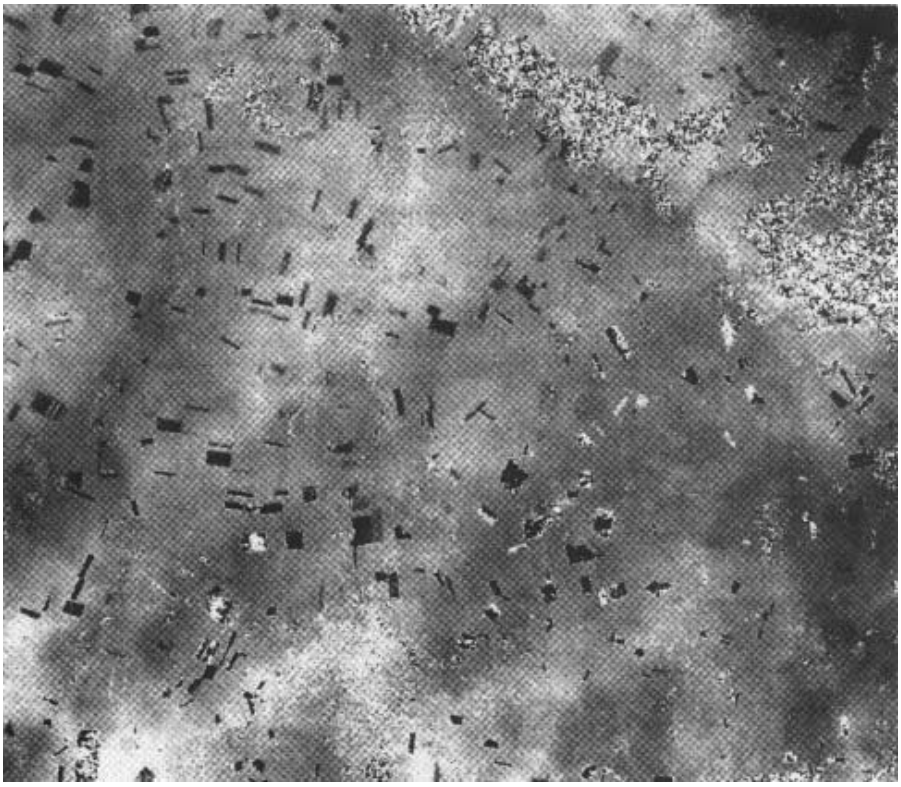

Figure 6: Phase image of the area south of Bonn with clear field structures due to farmer activities.

3. PROBLEMS

There are still more problems:

- The uncertainty of the baseline can lead to errors, because the reference fringes depend strongly on B when calculating the reference plane for the DEM estimation.
- The relationship between range and phase is given by the velocity of light c. As the line of sight to the pixel passes the ionosphere and the troposphere, the propagation velocity can vary and the range measurement will contain some error.
- A local rain cell can temporally change the soil moisture and the penetration of waves into the surface. Regional errors can be the result.

4. COHERENCE OF INTERFEROMETRIC IMAGE PAIRS

The interferometry requires very precise image matching of the pair of images to 1/10th of a pixel, for example. If this is not done perfectly, then the fringes will not show up or will be noisy. This strongly affects the unwrapping of the fringes for the generation of a DEM. To control the registration of a image pair the correlation factor for a set of corresponding pixels is estimated.
However, coherence is an information in itself. If a field is ploughed during the time between the first and the second image, then the coherence will be reduced, and if it is densified, then also the average height might change. Both effects can show up, the first effect in the "coherence image", the second one in the phase image (figure 6).

5. SETS OF IMAGES

If more than just two images takes are available, then one can separate the various effects. As an example it is shown in fig. that the use of image sets with different baselines, at different periods,

'Photogrammetric Week '95', D. Fritsch & D. Hobbie, Eds., Wichmann Verlag, Heidelberg, 1995

with different geometry (applying both, sets of images from the ascending orbits and also sets of images from descending images) can help to determine topography, horizontal motion of ice (ice stream) and vertical motion (tides) (figure 7).

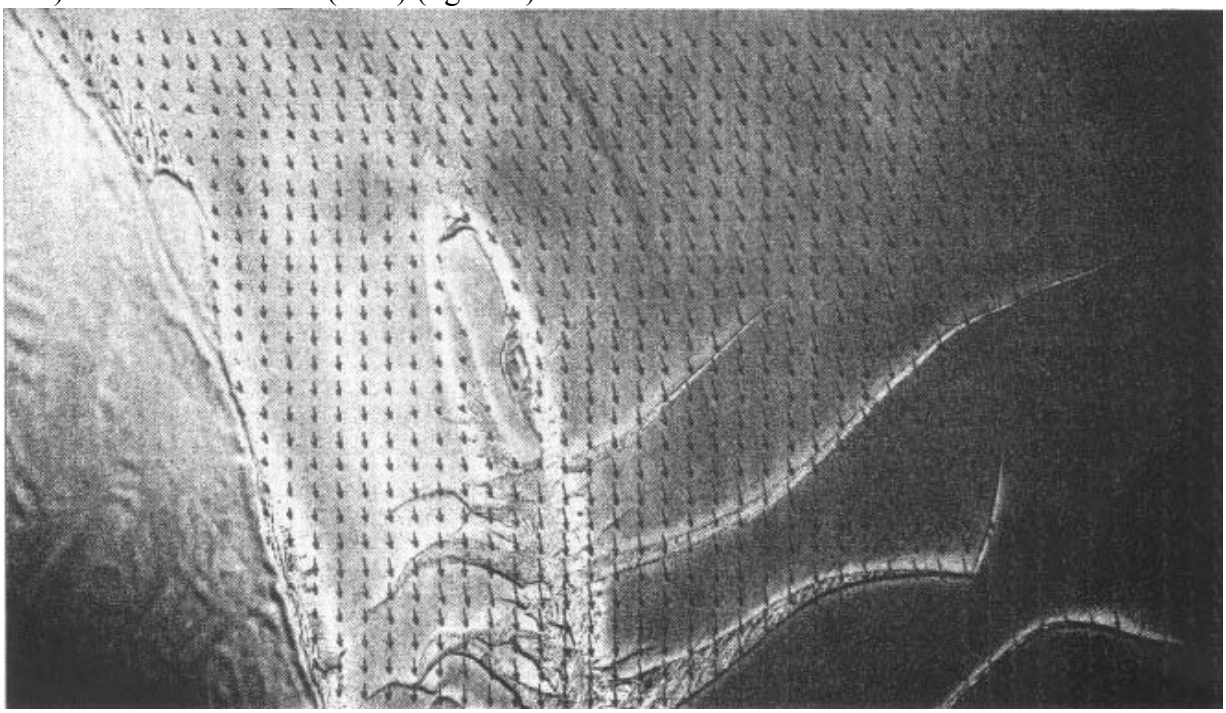

Figure 7: Estimation of horizontal ice motion of the shelf ice in Antarctica.

Monitoring of geodynamically active zones will lead to the observation of motions concerning earthquakes by comparing images before and after the event. One has to imagine that effects of earthquakes, which can cause surface shifts out to 100 km from epicentre in the order of cm, can be detected by the interferometry with a noise level of one to two mm in arid areas [Massonet et al.].
In volcanology it is interesting that the "growing" of the surface before an event can be detected with sub-cm precision. Monitoring surface stress before the occurrence of geodynamic activities and deriving models, allowing some sort of prediction is a highly important task.

6. TANDEM MISSION

It is quite obvious that application of a single satellite requires compromises: Very short repeat periods can be achieved for only very small fractions of the earth. Full coverage of the earth requires on the other side long time intervals between the first and the second image take. ERS-1 had for some time the 3-day repeat orbit, which was extremely valuable for the interferometry, and had also the 35 day repeat orbit for a (nearly) full coverage of the earth.
Now, with the availability of the ERS-2 ESA has planned the tandem mission for one year: The two satellites will fly 35-day repeats orbits, but the second satellite will take the image of the same scene 1 day after the first one. So, one can acquire within 35 days a complete earth coverage with a 1 day time interval (figure 8).

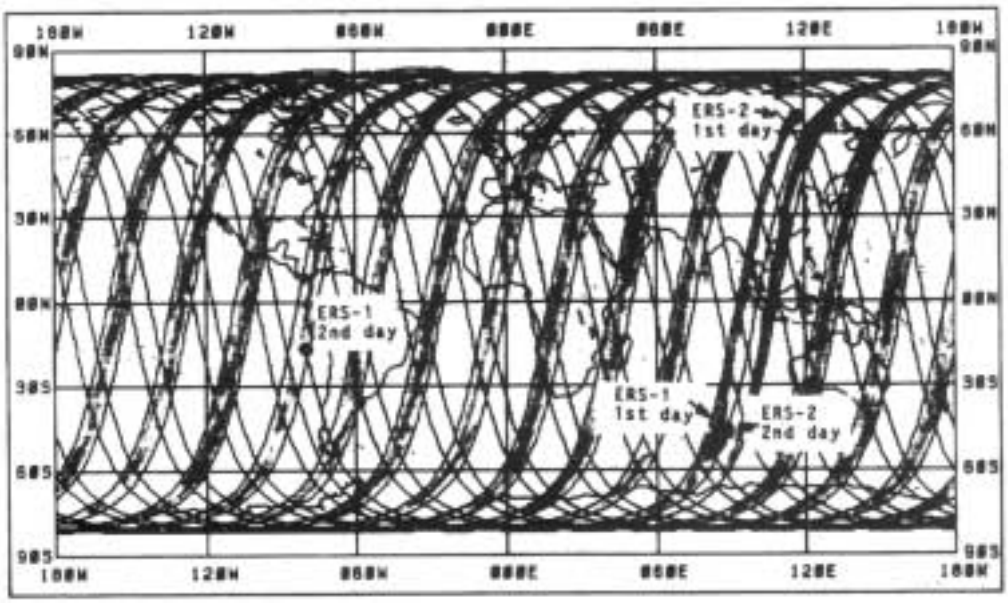

Figure 8: Footprint of ERS-1 and ERS-2 in planed TANDEM configuration. ERS-2 uses the same orbit and maps the same area with one day delay.

7. REAL BASELINE INTERFEROMETRY

For the next flight of the X-SAR/SIR-C experiment the German/Italian X-SAR will apply a boom and install a second receiving SAR unit. This allows to acquire simultaneously both images with a fixed antenna distance. This will offer a new quantum jump for DEM generation, because there is absolute no surface change, only the very small difference in the inclination angle caused by the distance between the two antennae (figure 9).

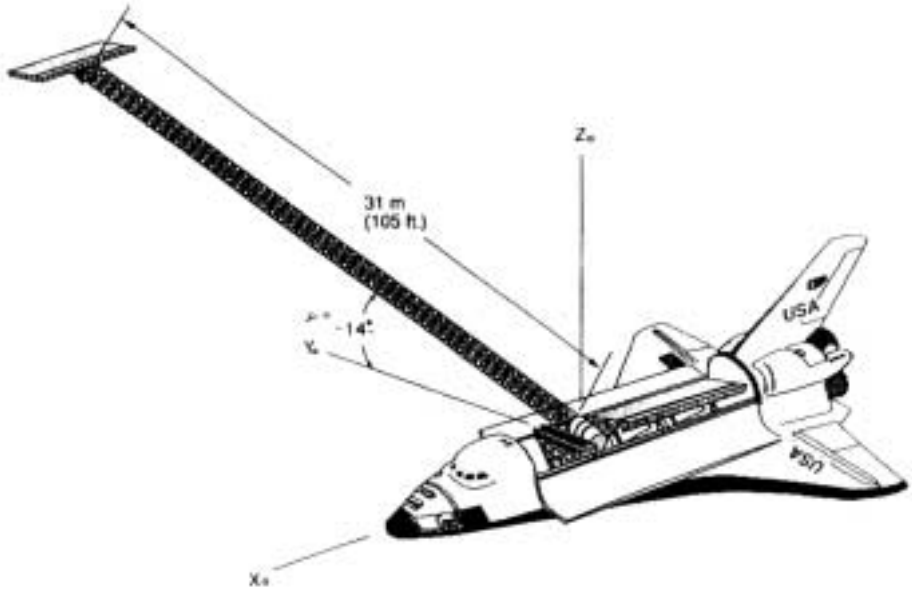

Figure 9: SAR system with two antennae for simultaneous data aquisition from the same area.

8. CONCLUSIONS

The SAR-techniques offers a lot of new possibilities to apply remote sensing for scientific and practical purposes. SAR- interferometry is of particular interest, but it is still in a development status. It needs

'Photogrammetric Week '95', D. Fritsch & D. Hobbie, Eds., Wichmann Verlag, Heidelberg, 1995

both, further development of the space segment and further investigations before the operational use for the different applications is established. But the achieved results concerning DEM generation and change detection are promising.

9. REFERENCES

Prati, C. and F. Rocca (1990): Limits to the resolution of elevation maps from stereo SAR images. Int. J. Remote Sensing, Vol.11, No.12, pp. 2215-2235.

Hartl, P. and K.-H. Thiel (1993): Bestimmung von topographischen Feinstrukturen mit interferometrischem ERS-1-SAR. Zeitschrift für Photogrammetrie und Fernerkundung, Vol., 3, pp. 108-114.

Hartl, P. and K.-H. Thiel (1993): Fields of Experiments in ERS-1 SAR Interferometry in Bonn and Napex. International Symposium - From Optics to Radar, SPOT and ERS-1 Applications, Paris 10th-13th May, 1993.

Massonnet, D., C. Carmona, and M. Rossi (1993): An Earthquake Test Site Studied by Differential Interferometry. International Symposium - From Optics to Radar, SPOT and ERS-1-Applications, Paris, 10-13th May 1993.

Schreier, G. (1993): SAR Geocoding: Data and Systems. Editor, Wichmann Verlag.

Hartl, P., K.-H. Thiel, X. Wu, C. Doake and J. Sievers (1994): Application of SAR interferometry with ERS-1 in the Antarctic. Earth Observation Quaterly, N^0 43-March1994, European Space Agency, ISSN 0256-596X.